Antibacterial Photodynamic therapy by zinc phthalocyanine against multi-drug resistant *Pseudomonas aeruginosa* in burn infection

Forouhe Kiyani [1], Fereshte Ghandehari[1]*, Mahnoosh Fatemi[2], Malahat Rezaee [3], Ali-Mohammad Ahadi[4]

1- Department of Microbiology, Fal.C., Islamic Azad University, Isfahan, Iran
2- Department of Biology, Fal.C., Islamic Azad University, Isfahan, Iran
3- Department of Biochemistry , Fal.C., Islamic Azad University, Isfahan, Iran
4- Department of Genetics, Faculty of Science, Shahrekord University, Shahrekord, Iran

* Corresponding: Fereshte Ghandehari.
.
Tel: +983137420140
 Email: fe_gh_2010@yahoo.com
Fe.ghandehari@iau.ac.ir

Abstract

Due to the prevalence of MDR strains, alternative treatments, such as antimicrobial photodynamic therapy (aPDT), have received much attention. This technique is an interactive technology that works with the help of photosensitizers and through the production of active oxygen radicals. This study aimed to investigate the effectiveness of aPDT against multi-drug *Pseudomonas aeruginosa* resistant bacteria using nanoemulsion containing zinc phthalocyanine (NE/ ZnPc) in a burn wound model in *in vitro* and *in vivo* conditions.Optimization of photodynamic therapy conditions in different drug concentrations, different incubation times, different doses of laser radiation was performed *in vitro*, and then the anti-biofilm effects of the optimal concentration against clinical isolates of *P. aeruginosa* resistant to several drugs were investigated. *In vivo* conditions, male rats were divided in 7 groups: control, burn wound group, bacterial infected burn wound, infected burn wound and laser treatment, infected wound and treatment with laser and drug (optimal concentration), infected wound and treatment with drug alone, infected wound and treatment with nanoemulsion alone. The area of the burn wound was measured at the beginning and end of the test. Pieces of skin tissue were collected in order to perform histological studies and measure the expression of EGFR and SOD1 genes.

Based on the results, the drug in concentration of 40 μg/ml encapsulated in nanoemulsion , the laser dose of 13 J/cm2 and the incubation time of 2 hours were selected as optimal conditions. Under these conditions, 80% biofilm inhibition was observed. According to the histological results, NE/ ZNPc-mediated aPDT and laser radiation reduced the burn wound area and significantly accelerated the wound healing process, as well as increasing EGFR gene expression and decreasing SOD1 gene expression to normal levels.

the promising antibacterial and anti-biofilm activity of NE/ClZNlPc-mediated aPDT against MDR *P. aeruginosa* bacteria and the increased expression of EGFR and SOD1 in the infected

wounds of rats indicate that this treatment may be used as an alternative treatment to eradicate bacteria with Multidrug resistance.

Keyword: nanoemulsion, aPDT, photosensitizers, zinc petalocyanine

1. Introduction: Burns are the fourth most common cause of trauma worldwide. In extensive and deep burns, the immune system is weakened, making patients susceptible to invasive bacterial infections, leading to serious complications such as sepsis and toxic shock syndrome. Studies on burn wounds for determining bacterial profiles and antibiotic susceptibility of isolates have shown that *Pseudomonas aeruginosa* is one of the most common isolates in burn wounds, and many of these isolates exhibit antimicrobial resistance. This bacterium, through the production of various virulence factors, plays a role in the establishment of invasive infections (1 , 2). In addition to antimicrobial resistance, *P. aeruginosa* ability to form biofilms is considered a protective mechanism against physical, chemical, and environmental stresses (3,4). In burn infections, the pathophysiology of burn trauma is altered, so the dose and choice of antibiotic for treatment varies from person to person. On the other hand, inappropriate antibiotic prescription can lead to increased antibiotic resistance and the growth of multidrug-resistant bacteria(5). Therefore, currently, one of the best alternative treatments to antibiotics for infections caused by this bacterium is photodynamic therapy (PDT). This technique offers a promising approach to killing antibiotic-resistant bacteria using multiple light sources and photosensitizing dyes to reduce the number of Gram-positive and Gram-negative bacteria. The mechanisms responsible for bacterial damage via PDT include DNA damage, cell membrane degradation, and alteration of membrane proteins, potassium ion leakage, and overall cell structure disruption (6). The basis of PDT involves inducing oxidative stress by exposing a photosensitizing drug to light. In this approach, active oxygen species and free radicals weaken the microorganism's antioxidant defenses, ultimately leading to their elimination (7). Phthalocyanines are the most common and effective photosensitizers used in PDT due to their high absorption in the red light region. Because of their macrocyclic hydrophobic structure, phthalocyanines tend to aggregate in biological solutions. Thus, there is a need for systems that encapsulate these drugs to protect them from metabolic breakdown, pH changes, or temperature fluctuations (8, 9). Nanoemulsions, due to their high stability, low toxicity, and gradual and sustained drug release potential, as well as their ability to deliver lipophilic compounds, are suitable systems for facilitating the transfer of drugs across the plasma membrane and intracellular delivery of lipophilic drugs (10).

Objectives: The aim of the present study is to evaluate the inhibitory effects of photodynamic therapy using zinc phthalocyanine in a nanoemulsion system against a clinical isolate of MDR Pseudomonas aeruginosa obtained from burn infections under in vitro and in vivo conditions.

2. Materials and Methods:

2.1. Isolation and Identification of *P .aeruginosa* Strains from Burn Infections

In this study, 30 *P .aeruginosa* isolates were collected from burn wounds of patients hospitalized at Taleghani Burn Hospital in Ahvaz. The isolates were identified using biochemical tests. The confirmed isolates were stored in LB broth (Merck, Darmstadt, Germany) medium containing 20% glycerol at -80°C.

2.2. *In Vitro* Studies

2.2.1. Determination of Antibiotic Resistance Patterns

According to the M100 protocol of the Clinical Laboratory Standards Institute (CLSI2022), 10 different antibiotics, including ceftazidime (30 μg), cefepime (30 μg), aztreonam (30 μg), imipenem (10 μg), meropenem (10 μg), amikacin (30 μg), ciprofloxacin (5 μg), piperacillin-tazobactam (100/10 μg), and gentamicin (10 μg), were selected (Padtan Teb Company).

 Antibiotic resistance patterns of the strains were determined using the Kirby-Bauer disk diffusion method on Mueller-Hinton agar (Merck, Darmstadt, Germany) with a standard turbidity of 0.5 McFarland. The standard *P. aeruginosa* strain ATCC 27853 was used for quality control.

2.2.2. Nanoemulsion preparation

For preparation of nanoemulsion containing Zinc Phthalocyanine (Sigma-Aldrich, Germany), hazelnut oil (Oseweh Company (Isfahan, Iran)) was used as the oil phase. Lipoid S75 (Lipoid, Germany) and PEG 40 (Kimyagaran Emrooz Chemical Industries Co., Iran), were applied as surfactants. The spontaneous emulsification method was used for nanoemulsion preparation. In our previous study (results not shown), different ratios of oil and surfactants were examined to get the most stable nanoemulsion. The most appropriate values of ingredients were Lipoid S75:PEG (1:1), and a O/S ratio of 0.75. O/S ratio was fixed for the preparation of nanoemulsions with different concentrations of ZnPc. At first, ZnPc was dissolved in ethanol at a concentration of 13.8 mM as a stock solution. Then, different volumes of the ZnPc solution were added to the oil-surfactants mixture to achieve a ZnPc concentration range of 10-80 µg/ml. Ethanol was then removed at 100 °C. In the final step, water was added dropwise and homogenized under simple stirring to obtain an equilibrium state. Blank nanoemulsion was prepared through this same procedure without ZnPc.

2.2.3. Optimization of Photodynamic Therapy Conditions

Optimization of photodynamic therapy conditions including drug concentrations, incubation times, and laser doses was performed as one factor at a time optimization method during three steps. In each step, optimization of a factor in various ranges of values was carried out while two other factors kept constant at a certain value. Subsequently, 300 microliters of NE/ZNlPc at drug concentrations of 0, 10, 20, 40, 80 µg/ml were added to wells containing bacteria (OD600 = 0.55-0.06) and incubated for 30 minutes in the dark at 37°C. Following the incubation period, the wells were exposed to a laser with a dose of 13 J/cm². To select the optimal incubation time,

bacterial plates with the optimized drug concentration, achieved from the previous step, were incubated in the dark for 30 minutes, 1 hour, 2 hours, and 4 hours. In the next step, the bacterial plates with the optimized drug concentration and optimal incubation time were exposed to laser doses of 6, 13, and 20 J/cm². Each experiment was repeated three times. The decimal logarithm of CFU/ml was counted and normalized with respect to the CFU/ml of control cells (untreated).

2.2.4. Biofilm inhibition assay

100µl of suspension of *P .aeruginosa* was added into 96 well titre plates. The conditions tested were: 1) control which contained bacteria (B), 2) Bacteria exposed to optimal laser dose(B,L+), 3) Bacteria treated with optimal drug concentration without laser (B,d+,l-) , 4) Bacteria treated with optimal drug concentration with laser (B,d+,l+),5) Bacteria under nanoemulsion treatment without laser(B,N+,L-) and 6) Bacteria under nanoemulsion treatment with laser(B,N+,L+). Plates were incubated at 37^{oc}. After the incubation, the liquid suspension was removed and 100 µl of 1% w/v aqueous solution of crystal violet was added. Following staining at room temperature for 30 minutes the dye was removed and the wells were washed thoroughly, 95% ethanol was added and incubated for 15 minutes (11). The reaction mixture was read spectrophotometrically at 570nm. Inhibition mediated reduction of biofilm formation was calculated by the following formula:

- % inhibition biofilm = $\dfrac{\text{OD in control} - \text{OD in treatment} \times 100}{\text{OD in control}}$

2.3. *In Vivo* Studies

2.3.1. Animal Grouping

42 male rats (250±15 g) were obtained and kept at 20±2°C, a humidity of 50 ±5%, and 12–12 hour's light/dark cycle and access to food and water *ad libitum*. The rats were divided into seven groups as follows: control group (no wound), burn wound group, burn-infected group with MDR *P. aeruginosa*, infected wound group treated with laser, infected wound group treated with laser and NE/ZNlPc (at optimal drug concentration), infected wound group treated with NE/ZNlP without laser, and infected wound group treated with the of nanoemulsion.

2.3.2. Burn Infection Modeling in Experimental Groups

After shaving the back area and anesthetizing the rats using ketamine at a concentration of 100 mg/kg, a second-degree burn was induced on the back using a hot metal rod (100±2°C) with a diameter of 2×2 cm (12). Histopathological changes, including burn depth, were assessed by H&E staining and confirmed by a pathologist in a pilot study. The initial wound diameter was measured using calipers. Subsequently, the wounds were infected with 300 µl of a microbial suspension with a concentration of 1.5×10^8 CFU/ml, and the rats were then transferred to completely sterile cages.

2.3.3. Photodynamic Therapy for Burn Wounds After confirming infection in the wounds, the groups were treated with the optimized conditions of photodynamic therapy as described above for seven consecutive days. At the end of the treatment period, the wound area was measured using Vernier calipers. The results were compared between the groups at the end of the test.

2.3.4. Histopathological Studies

A portion of the skin tissue from the control group and the burn sites of other groups were isolated and underwent dehydration, clearing, embedding, sectioning using a microtome, and staining with hematoxylin and eosin. Finally, the slides were examined under a light microscope.

2.3.5. Gene Expression Analysis Using Real-Time PCR

RNA extraction was performed using Trizol solution according the company manual, and its concentration was measured by spectrophotometry, while integrity was assessed via gel electrophoresis. cDNA synthesis was conducted using the Sinaclon kit (RT5201) according to the specified protocol. Relative Realtime RT-PCR was optimized based on $2^{-\Delta\Delta Ct}$ method (13). Samples were gently mixed without vortexing and placed in the real-time PCR device. The first stage included one cycle at 95°C for 5 seconds, the second stage involved one cycle at 95°C for 10 minutes, and the third stage comprised 40 cycles at 60°C for 30 seconds for denaturation, primer annealing, and extension. Primer sequences are listed in Table 1.RNA extraction was performed using the Trizol method, and its concentration was measured by spectrophotometry, while integrity was assessed via gel electrophoresis. cDNA synthesis was conducted using the Sinaclon kit (RT5201) according to the specified protocol. Samples were gently mixed without vortexing and placed in the real-time PCR device. The first stage included one cycle at 95°C for 5 seconds, the second stage involved one cycle at 95°C for 10 minutes, and the third stage comprised 40 cycles at 60°C for 30 seconds for denaturation, primer annealing, and extension(14). Primer sequences are listed in Table 1.

Table 1: Sequence of primers used in real-time PCR

| Gene	Sequence (5′-3′)	Size (bp)	NCBI Accession number
SOD1	F'-GAAGAGAGGCATGTTGGAGAC R: ACCACTGTACGGCCAATGATG	125	(NM_011434.24)
β-actin (Control)	F: - GGACTCCTATGTGGGTGACG R: - AGGTGTGGTGCCAGATCTTC	119	NM_007393.5
EGFR	F: -GAGAACTGCCAGAAATTGACC R: GTACACCCCGCAGCACATTG	110	NM_207655.2

.2.4. Statistical analysis

All data were expressed as mean ± standard deviation and analyzed using one-way analysis of variance (ANOVA) with SPSS version 22, with a significance level of p≤0.05. To statistically

analyze relative gene expression changes among different treatment groups compared to controls, GraphPad Prism (version 7) was used.

3. Results
3.1. In Vitro Studies

Selection of MDR Strain and Optimization of Photodynamic Therapy among the 30 clinical isolates of Pseudomonas aeruginosa, strain P18 demonstrated resistance to five different antibiotics from various classes. This isolate was chosen for further experiments. Based on the optimization results (Figure 1), the optimal conditions were determined as a drug concentration of 40 µg/ml, a laser dose of 13 J/cm², and an incubation time of 2 hours.
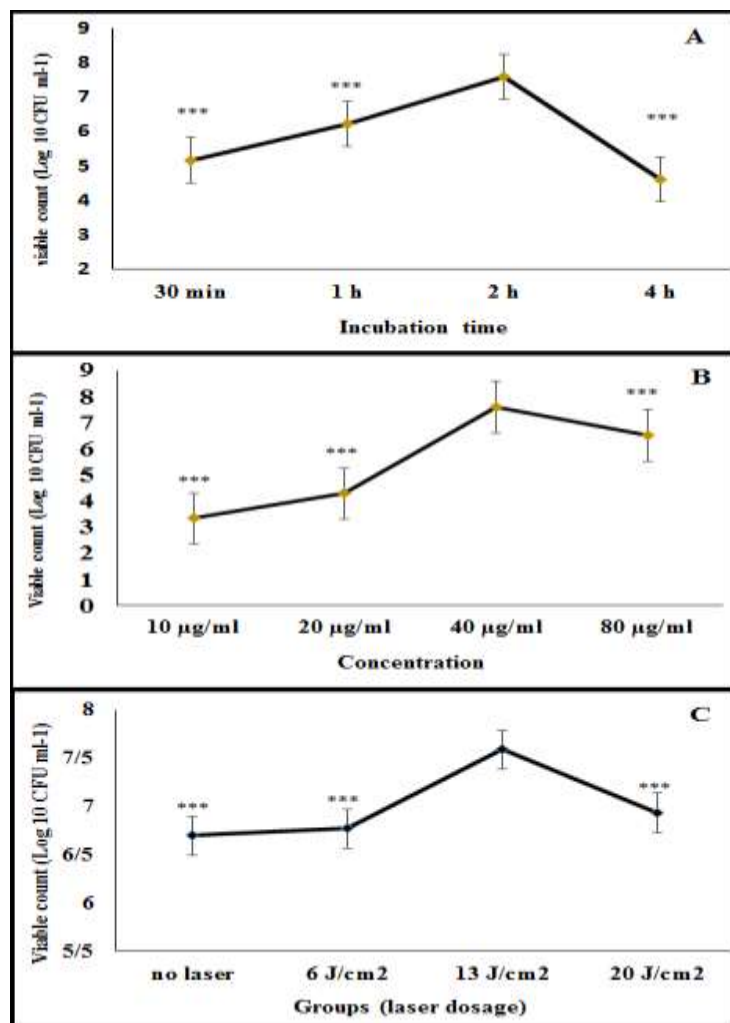
Figure 1: A Comparison of the effect of mean incubation times with a drug concentration of 40 µg/mL and a laser dose of 13 J/cm² on the viable count (Log 10 CFU ml^{-1}). **B:** Comparison of different drug concentrations with a 2-hour incubation time and a laser dose of 13 J/cm². **C:** Comparison of various laser doses with a drug concentration of 40 µg/mL and a 2-hour incubation time significant difference (*** p≤0.001).

3.2. Anti-Biofilm Effects of Photodynamic Therapy

The results of the anti-biofilm effects of zinc phthalocyanine (**Figure 2**) demonstrated that the combination of laser and NE/ZNlPc exhibited a significant increase in anti-biofilm activity compared to laser alone or blank nanoemulsion . This increase was notably more pronounced in the group treated with NE/ZNlPc under laser (P≤0.001). However, in the groups treated with nanoemulsion and the NE/ZNlPc without laser, there was no significant difference in biofilm inhibition percentage compared to the control group.
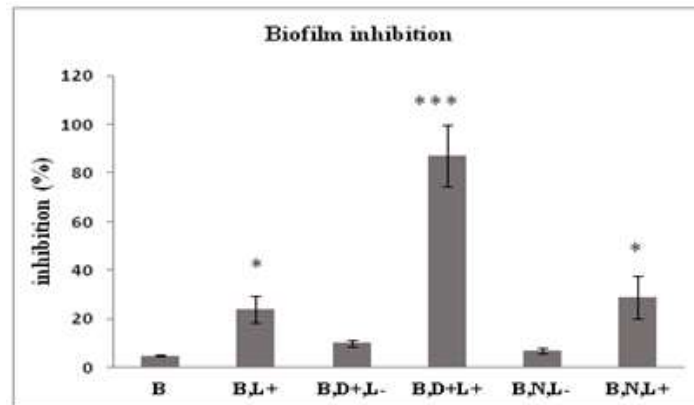

Figure 2: Comparison of biofilm inhibition percentage between experimental groups. Data are expressed as mean ± SD. Significance levels include ***p≤0.001**, **p≤0.01,** *p≤0.05.*

*B:*Control which contained bacteria. B,L+: Bacteria exposed to optimal laser dose. B,D+,L-: Bacteria treated with optimal drug concentration without laser.   B, D+, L+: Bacteria treated with optimal drug concentration with laser. B,N+,L-: Bacteria under nanoemulsion treatment without laser. B,N+,L+: Bacteria under nanoemulsion treatment with laser

3.3. In Vivo Study Results

3.3.1. Comparison of Burn Wound Diameter in Experimental Groups

According to Figure 3, at the end of the study a reduction in wound diameter was observed only in the group of rats treated with NE/ZNlPc under laser compared to the burn wound group (p≤0.001). These findings indicated that the wound diameter in this group was significantly smaller compared to all other groups (p≤0.001).
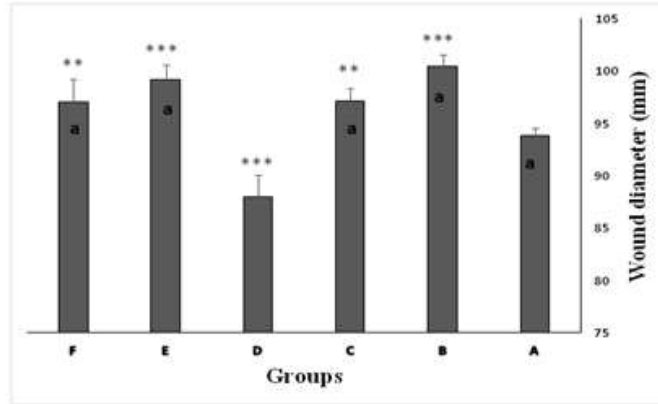
Figure 3: Burn wound diameter of experimental groups at the end of the test period data are expressed as mean ± standard deviation. *a* indicates p≤0.001 compared to experimental groups treated with the NE/ZNlPc under laser exposure. Stars represent comparisons of other groups with the burn-only group*** *.p≤0.001*, **p≤0.01 , *p≤0.05.*

3.3.2. Histopathological Examination

In the control group (Figure4: A1,A2), all major layers of the skin, including the epidermis, dermis, and hypodermis, were clearly identifiable, along with normal hair follicles, blood vessels, and sebaceous glands. In the burn wound group (B1), the epidermis was completely absent, and collagen fibers in the dermis appeared homogeneously aligned. At higher magnification (B2), numerous blisters were observed in the dermis. In groups with infected burn wounds (C1), there was a complete loss of the epidermis, bacterial colonies on the surface layer, and extensive dermal damage (C2), along with inflammatory cell infiltration from the subcutaneous to the muscle layers (C3).

In the group with infected wounds treated only with the drug (D1), the epidermis was still absent, with extensive dermal damage, hyperemia, bacterial colonies, and homogeneously arranged collagen fibers (D2). Similarly, in the group treated with nanoemulsion alone (E1), the epidermis did not form, while hyperemia, homogeneously arranged collagen fibers, and extensive inflammatory cell infiltration in the hypodermis and underlying dermal layers were observed (E2).In the infected burn wound group treated with laser exposure, a thin epidermal layer was present, though hair follicles and dermal papillae were still absent (F1). At higher magnification, collagen fibers exhibited a relatively normal arrangement, but inflammatory cells were still observed in the subcutaneous and muscle layers (F2, F3). Significant improvement was observed following burn treatment with both the drug and the nanoemulsion (G1). The epidermal thickness was similar to that of the control group, with the presence of hair follicles and dermal papillae. Other layers appeared normal, with visible, normally arranged hair follicles and collagen, and a decrease in inflammatory cells in the hypodermis (G2, G3).
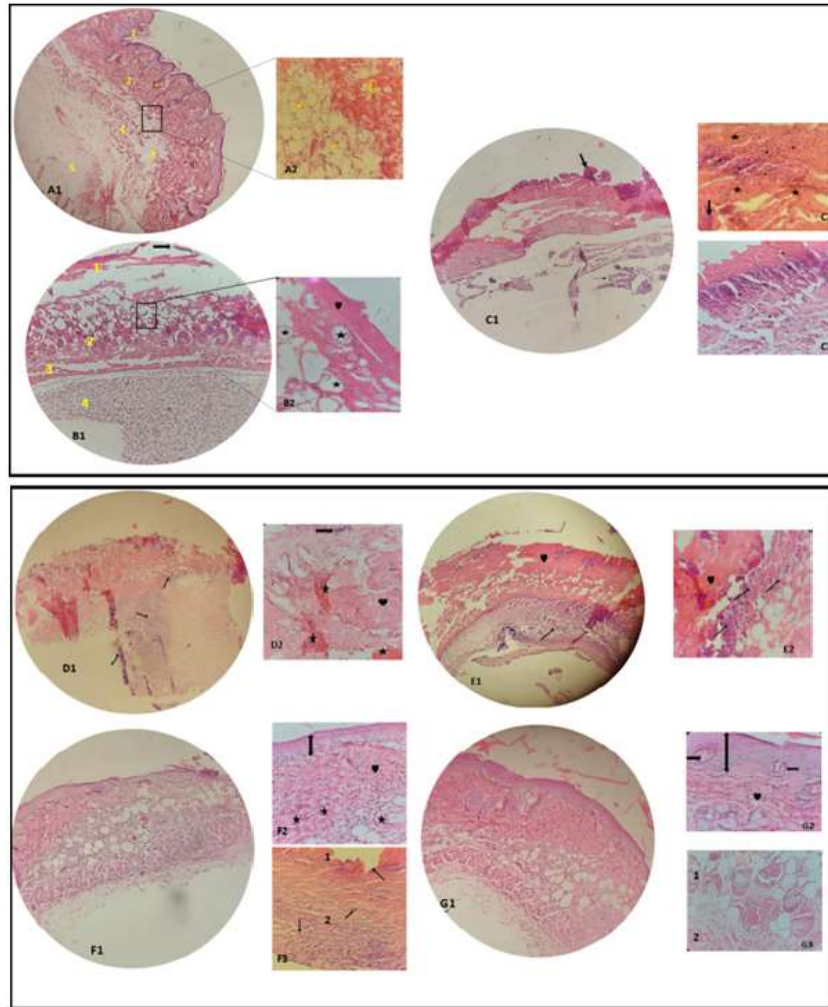
Figure 4: Histological Sections of Skin Tissue in Control and Experimental Groups.

A1: Sections of control group skin tissue showing layers 1 to 5, corresponding to the epidermis, dermis, hypodermal adipose tissue, muscle tissue, and subcutaneous layer, respectively, with a completely normal structure at 40× magnification. The star symbol indicates a hair follicle. **A2**: Higher magnification (100×) image of normal skin tissue in the control group, illustrating normal collagen fibers (indicated by the arrow) and normal adipose tissue (indicated by the heart shape). **B1**: Sections of skin tissue from rats with induced burns. Layer 1 shows the dermis, with visible destruction and separation from the underlying layers 2 to 4 (hypodermis, muscle tissue, and subcutaneous layer). **B2**: Collagen fibers in a homogeneous arrangement (indicated by the heart) and fluid-filled blisters (indicated by the star) are visible in the dermal region at 100× magnification. **C1**: Skin tissue from the burn infection group, showing the complete absence of the epidermis, with bacterial colonies on the surface layer (indicated by the arrow) and extensive dermal damage at 40× magnification. **C2 and C3**: Sections from the burn infection group at 100× magnification. In **C2**, a thick arrow indicates bacterial colonies, a thin arrow marks invasive inflammatory cells in the dermis, and stars denote blood vessels. In **C3**, arrows illustrate the invasion of inflammatory cells from the subcutaneous layer toward the muscle layer.

Skin of the Burn Infection Treated with the Drug**: D1:** Similar to the previous group, the epidermis is not observed, and the dermis appears highly disordered with extensive damage. The arrows indicate

inflammatory cells. **D2:** Shows a bacterial colony (arrow), hyperemia (star), and homogenous collagen fibers. **E1:** The epidermis is still not visible, similar to the previous group. Inflammatory cells are widely present in the subcutaneous layer (arrow). The heart symbol indicates homogenous collagen fibers. **E2:** At higher magnification, the presence of inflammatory cells in the hypodermis and deeper dermal areas is evident. The bacterial colony and hyperemia in tissue slides from this group were less prominent than in previous groups.

Skin of the Burn-Infected Group Treated with Laser: **F1:** The epidermal layer is visible, and other layers appear almost normal. **F2:** The double-headed arrow indicates a thin epidermis; hair follicles and dermal papillae are still not observed in this layer. Stars represent hyperemia, and the heart symbol indicates collagen fibers with a relatively normal arrangement. **F3:** Arrows indicate the presence of inflammatory cells in the subcutaneous (2) and muscle (1) layers.

Skin of the Burn-Infected Group Treated with NE/ZNlPc and Laser. **G1:** This figure shows an epidermis with a thickness close to the control group, along with the presence of hair follicles and dermal papillae; other layers appear normal. **G2:** The double-headed arrow shows the thickness of the epidermis. Arrows indicate cross-sections of hair follicles, and the heart symbol represents the normal arrangement of collagen. **G3:** Numbers 1 and 2 represent the hypodermis and muscle layer, respectively, with a very low number of inflammatory cells in these areas.

3.3.3. EGFR and SOD 1Gene Expression Changes in Experimental Groups:

The results of the comparison of EGFR gene expression between experimental groups and the control group revealed a significant increase (**Figure 5A**). This increase was particularly prominent in groups B, D, and E, especially in group E (*p≤0.001*).
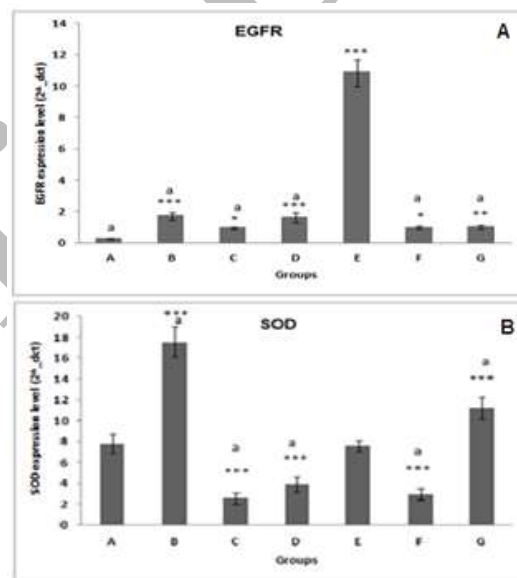
Figure 5 - Analysis of EGFR (A) and SOD 1(B) Gene Expression Changes in Groups: Data are presented as mean ± SD. Stars indicate comparisons between the control group and other groups, while "a" denotes comparisons of Group E with other groups at the p≤0.001 level. Significance levels are as follows: p≤0.001***, p≤0.01**, p≤0.05*. Groups A to G are as follows: Control group, Burn group, Burn

Infection group, Laser-treated group, NE/ZNlPc treated under Laser, Drug-treated group, and Nanoemulsion-treated group.

According to the **Figure 5B**, SOD1expression increased in Groups B and G, while significant decreases (p≤0.001) were observed in Groups C, D, and F. Upon comparing the group treated with NE/ZNlPc under laser with other groups, no significant difference in the expression level of this gene was observed compared to the control group.

4. Discussion: Treatment of burn wound infections is a major medical challenge. A high percentage of mortality in burn units is due to post-incident infections, with P. *aeruginosa* being the most prevalent colonizing pathogen in burn wounds. The main issue in treating these infections is the formation of multiple biofilms resistant to most available treatments. Antibiotic treatment can have side effects, posing a threat to burn patients' health. For deep burn wounds, antibiotic use may inhibit skin tissue regeneration and edema treatment. Thus, the development of new antibacterial therapies, especially for burn infections caused by multidrug-resistant bacteria, is crucial. Increasing microbial resistance to antimicrobial compounds necessitates the exploration of new therapeutic approaches for bacterial infections.

One promising approach is antimicrobial photodynamic therapy (aPDT), which is effective against multidrug-resistant (MDR) bacteria (15). The technique relies on inducing oxidative stress by exposing a photosensitizing drug to laser radiation. Optimization of this method was performed using NE/ZNlPc at different concentrations, various laser doses, and incubation times on *P.aeruginosa* isolates from patients with burn wounds and MDR strains. The results showed that the highest inhibitory effect was achieved with 40 µg/mL of the drug, 2-hour incubation time, and 13 J/cm² laser dose. Additionally, the anti-biofilm effect of the optimized conditions was examined on the target isolate. The findings indicated that while laser treatment and nanoemulsion alone increased biofilm inhibition, the highest inhibition percentage was observed in the group treated with both the drug and laser.The results of antibacterial photodynamic studies by Anjou et al. (16) using carbon nanotubes conjugated with malachite green dye and irradiated for 3 minutes with red laser at a 660 nm wavelength showed growth and biofilm inhibition in *P. aeruginosa* and *Staphylococcus aureus* strains. Ribeiro and colleagues, using photodynamic therapy with curcumin extract on methicillin-resistant *S. aureus* biofilm, observed a significant reduction in biofilm inhibition. SEM micrograph evaluations also demonstrated a reduction in bacterial cells and extracellular polymeric matrix after PDT. It appears that the zinc phthalocyanine nanoemulsion, due to its small size, can penetrate bacterial cells even within biofilm clusters, potentially disrupting metabolic activity and inhibiting bacterial cell growth(17).In continuation of this research, the optimal drug concentration, incubation time, and laser dose were evaluated in vivo on burn infections in rats**. The results of wound diameter comparisons among the experimental groups after the treatment period revealed a significant reduction in wound size in the group of rats treated with drug-containing nanoemulsion under laser irradiation compared to other groups, aligning with histopathological studies. Histopathological analysis is considered the gold standard for assessing wound healing progress and determining epidermal epithelialization. The skin is the most critical barrier for human resistance against external invasion. Wound healing after skin injuries, such as burns, involves a complex series of processes, including cell proliferation and migration, cytokine secretion, and inflammatory responses (18). Inflammation represents the initial stage of wound healing and occurs nearly concurrently with hemostasis. As the inflammatory response overlaps, various cytokines and

growth factors activate and induce the proliferation, migration, and differentiation of repair cells, leading to biological behaviors such as epithelialization, angiogenesis, and collagen deposition. Continuous tissue remodeling, with fibroblasts differentiating into myofibroblasts, contributes to wound contraction and restoration of skin integrity (19).Bacterial infections can prolong the inflammatory phase, disrupt epithelial layer formation, collagen deposition, and ultimately impair wound healing (20). Previous studies have demonstrated the positive impact of photodynamic therapy (PDT) on tissue healing and repair in infected wounds (21,22). In the present study, the control group's tissue structure appeared completely normal, with appropriately thick dermis, epidermis, and hypodermis layers, including hair follicles, sebaceous glands, and blood vessels. In the burn wound group, epidermal destruction and numerous blisters and collagen fiber disarray were evident in the affected area. In the group with burn wounds infected by *P. aeruginosa*, there was more severe destruction of the epidermal and dermal layers, with numerous *P. aeruginosa* colonies and inflammatory cell invasion.In this study, zinc phthalocyanine's penetration was enhanced by the nanoemulsion system, likely resulting in deeper infection clearance from tissue surfaces and faster healing. Supporting this, Sarker et al. reported that antibacterial photodynamic therapy combined with antibiotics had beneficial effects in accelerating third-degree burn healing in mice infected with bacteria. These treatments stimulate macrophages to release chemical mediators, cytokines, and growth factors, which, in turn, enhance connective tissue production and generate new blood vessel sources to nourish and promote wound regeneration.**Results from Figueiredo-Godoi and colleagues on photodynamic therapy using methylene blue sensitizer on *Acinetobacter baumannii*-infected burns** also indicated this sensitizer's potential to penetrate the cell wall of Gram-negative bacteria, ultimately inhibiting and improving wound healing(23).In the present study, following burn induction, the SOD 1expression level significantly increased. However, after inducing infection in the wound, the expression level of this enzyme decreased. In the two infected groups treated with laser alone or drug alone, the enzyme level also decreased. Consistent with this study, antioxidant enzyme activity was also found to decrease in diabetic rats with infected wounds compared to the control group (7). Superoxide dismutase is the most important and primary antioxidant enzyme in all aerobic organisms, playing a key role in directly reducing reactive oxygen metabolites and serving as the first line of defense against superoxide radicals (O2-), converting superoxide anions to H2O2 and repairing cells. Previous research has shown that SOD 1levels increase during wound healing and accelerate the healing process (24, 25).Therefore; it appears that the reduction in enzyme expression following infection is due to increased oxidative stress caused by the overproduction of free radicals, which leads to the oxidation and subsequent denaturation of the enzyme. It seems that laser or drug alone did not have a significant effect on reducing oxidative stress. Photodynamic therapy (PDT) increases oxidative stress in bacteria, leading to their elimination, thereby this process prevents the immune system cells from engaging the bacteria in a violent fight. In this study, PDT using a NE/ZNlPc under laser irradiation brought the SOD 1enzyme expression level closer to normal During wound healing, various inflammatory cells such as neutrophils, macrophages, endothelial cells, and fibroblasts produce reactive oxygen species, which can increase the levels of these radicals and cause significant cell damage. Enhancing the body's antioxidant system can help reduce these radicals and facilitate the healing process (26). In the study by Kalyay and et al wounds induced in rats were treated with EGF therapy. The levels of thiobarbituric acid reactive substances (TBARS) decreased, while ascorbic acid, glutathione, and SOD activity levels increased, especially on the fifth day after treatment, gradually returning to normal by day 15.

These researchers suggested that EGF may act like an antioxidant, consuming toxic oxidative compounds, enhancing endogenous antioxidants, and ultimately promoting wound healing (27). Given the possible link between growth factors and antioxidants, the expression level of EGFR was also evaluated in skin tissue in this study. EGFR is a glycoprotein with tyrosine kinase activity and plays a vital role in controlling cellular signaling pathways. This tyrosine kinase receptor (RTK) belongs to the larger family of ErbB proto-oncogenes and is involved in cell survival, proliferation, angiogenesis, and invasion. EGF plays an important role in wound healing in the skin, cornea, oral mucosa, and stomach (28, 29). Numerous studies have highlighted the positive effects of growth factors on improving and restoring this factor in the healing of skin wounds in animals (28, 30). EGFR stimulates fibroblasts to synthesis VEGF and other growth factors involved in angiogensis, which promotes wound healing by reepitheliazation stimulation of angiogensis collagen deposition mypfibroblast differentiation, and extera matrix cell remodeling (30, 31). In the present study, EGFR expression levels increased in all experimental groups compared to the control group, with the highest increase observed in burn-infected rats treated with the drug-containing nanoemulsion exposed to laser. This suggests the potential impact of this therapeutic method on wound healing and histopathological results were consistent with these findings. The increased expression of EGFR and SOD 1in infected rat wounds following photodynamic therapy with NE/ZNlPc under laser irradiation (under optimal conditions) demonstrates the positive impact of this therapeutic method in the present study. Given the observed re-epithelialization along with neovascularization and reduced inflammation in tissue samples, this approach may serve as an alternative to antibiotic treatments for burn infections.

Authors' Contribution
Study concept and design: F.GH, F.K and M.F
Acquisition of data: F.GH, F.K and M.F
Analysis and interpretation of data: M.R, F.GH and M.F
Drafting of the manuscript: F.GH, F.K and M.F
Critical revision of the manuscript: F.GH, F.K, AM.A and M.F
Statistical analysis: M.F and M.R

Ethics
All procedures were carried out according to guidelines for working with laboratory animals, approved by the Ethics Committee of Islamic Azad University, Falavarjan branch, under the code IR.IAU.FALA.REC.13933.046.

Conflict of Interest
The authors declare that there is no conflict of interests

Data Availability
The data that support the findings of this study are available on request from the corresponding author.

Reference:

1- Spernovasilis, N., Psichogiou, M., & Poulakou, G. Skin manifestations of Pseudomonas aeruginosa infections. Current opinion in infectious diseases.2021; 34(2), 72–79. https://doi.org/10.1097/QCO.0000000000000717

2- Yang, T., Tan, Y., Zhang, W., Yang, W., Luo, J., Chen, L., Liu, H., Yang, G., & Lei, X. Effects of ALA-PDT on the Healing of Mouse Skin Wounds Infected With Pseudomonas aeruginosa and Its Related Mechanisms. Frontiers in cell and developmental biology.2020; 8, 585132. https://doi.org/10.3389/fcell.2020.585132

3- D'Arpa, P., Karna, S. L. R., Chen, T., & Leung, K. P. Pseudomonas aeruginosa transcriptome adaptations from colonization to biofilm infection of skin wounds. Scientific reports.2021; 11(1), 20632. https://doi.org/10.1038/s41598-021-00073-4

4- Kranjec, C., Morales Angeles, D., Torrissen Mårli, M., Fernández, L., García, P., Kjos, M., & Diep, D. B. Staphylococcal Biofilms: Challenges and Novel Therapeutic Perspectives. Antibiotics (Basel, Switzerland).2021; 10(2), 131. https://doi.org/10.3390/antibiotics10020131

5- Tsolakidis S, Freytag DL, Dovern E, Alharbi Z, Kim BS, Houschyar KS, Reumuth G, Schäfer B, Rennekampff HO, Pallua N, Grieb G. Infections in burn patients: a retrospective view over seven years. Medicina. 2022 Aug 8;58(8):1066

6- Badran, Z., Rahman, B., De Bonfils, P., Nun, P., Coeffard, V., & Verron, E. Antibacterial nanophotosensitizers in photodynamic therapy: An update. Drug discovery today.2023; 28(4), 103493. https://doi.org/10.1016/j.drudis.2023.103493

7- Sedeh, S. S., Fatemi, M., & Ghandehari, F. Antimicrobial Photodynamic Therapy Using Zinc Phthalocyanine Nanoemulsion Against Infected Wounds in Diabetic Rats. Avicenna Journal of Clinical Microbiology and Infection.2023; 10(3), 120-125. https://doi.org/10.34172/ajcmi.3496

8- Bunin, D. A., Martynov, A. G., Gvozdev, D. A., & Gorbunova, Y. G. Phthalocyanine aggregates in the photodynamic therapy: dogmas, controversies, and future prospects. Biophysical reviews.2023;15(5), 983–998. https://doi.org/10.1007/s12551-023-01129-7

9- Ömeroğlu, İ., & Durmuş, M. Water-soluble phthalocyanine photosensitizers for photodynamic therapy. Turkish journal of chemistry.2023; 47(5), 837–863. https://doi.org/10.55730/1300-0527.3583

10- Felifel, N. T., Sliem, M. A., Kamel, Z., Bojarska, J., Seadawy, M. G., Amin, R. M., & Elnagdy, S. M. Antimicrobial Photodynamic Therapy against Escherichia coli and Staphylococcus aureus Using Nanoemulsion-Encapsulated Zinc Phthalocyanine. *Microorganisms*.2023; *11*(5), 1143. https://doi.org/10.3390/microorganisms11051143

11- Namasivayam, S. K. R., & Roy, E. A. Anti biofilm effect of medicinal plant extracts against clinical isolate of biofilm of Escherichia coli. Int. J. Pharm. Pharm.2013; Sci, 5(2), 486-489.

12- Pavliuk, Bohdana, et al. "Therapeutic efficacy of the developed gel "Xeliogel" on a burn wound model in rats." Polski Merkuriusz Lekarski .2020; 331-334.

13- Livak KJ, Schmittgen TD. Analysis of relative gene expression data using real-time quantitative PCR and the 2(-Delta Delta C(T)) Method. Methods. 2001 Dec;25(4):402-8. doi: 10.1006/meth.2001.1262. PMID: 11846609

14- Tanaka, Y., Yamaguchi, A., Fujikawa, T., Sakuma, K., Morita, I., & Ishii, K. Expression of mRNA for specific fibroblast growth factors associates with that of the myogenic markers MyoD and proliferating cell nuclear antigen in regenerating and overloaded rat plantaris muscle. Acta physiologica (Oxford, England).2008; 194(2), 149–159. https://doi.org/10.1111/j.1748-1716.2008.01866.x

15- Feng, Y., Coradi Tonon, C., Ashraf, S., & Hasan, T. Photodynamic and antibiotic therapy in combination against bacterial infections: efficacy, determinants, mechanisms, and future perspectives. Advanced drug delivery reviews.2021; 177, 113941. https://doi.org/10.1016/j.addr.2021.113941.

16- Anju, V. T., Paramanantham, P., Siddhardha, B., Sruthil Lal, S. B., Sharan, A., Alyousef, A. A., Arshad, M., & Syed, A. Malachite green-conjugated multi-walled carbon nanotubes potentiate antimicrobial photodynamic inactivation of planktonic cells and biofilms of Pseudomonas aeruginosa and Staphylococcus aureus. International journal of nanomedicine.2019; 14, 3861–3874. https://doi.org/10.2147/IJN.S202734

17- Ribeiro, I. P., Pinto, J. G., Souza, B. M. N., Miñán, A. G., & Ferreira-Strixino, J. Antimicrobial photodynamic therapy with curcumin on methicillin-resistant Staphylococcus aureus biofilm. Photodiagnosis and photodynamic therapy.2022;37, 102729. https://doi.org/10.1016/j.pdpdt.2022.102729

18- Shpichka, A., Butnaru, D., Bezrukov, E. A., Sukhanov, R. B., Atala, A., Burdukovskii, V., Zhang, Y., & Timashev, P. Skin tissue regeneration for burn injury. Stem cell research & therapy2019; 10(1), 94. https://doi.org/10.1186/s13287-019-1203-3

19- Shi, Z., Yao, C., Shui, Y., Li, S., & Yan, H. Research progress on the mechanism of angiogenesis in wound repair and regeneration. Frontiers in Physiology2023; 14, 1284981. https://doi.org/10.3389/fphys.2023.1284981.

20- Lin, Y., Chen, Z., Liu, Y., Wang, J., Lv, W., & Peng, R. Recent Advances in Nano-Formulations for Skin Wound Repair Applications. Drug design, development and therapy.2022; 16, 2707–2728. https://doi.org/10.2147/DDDT.S375541

21- Gu, R., Fei, S., Liu, Z., Liu, X., Fang, X., Wu, H., Zhang, X., Xu, G., & Xu, F. Effects of photodynamic therapy in patients with infected skin ulcers: A meta-analysis. International wound journal.2024; 21(3), e14747. https://doi.org/10.1111/iwj.14747.

22- Tong, A., Tong, C., Fan, J., Shen, J., Yin, C., Wu, Z., ... & Liu, B. Prussian blue nano-enzyme-assisted photodynamic therapy effectively eradicates MRSA infection in diabetic mouse skin wounds. Biomaterials Science.2023; 11(18), 6342-6356. http://dx.doi.org/10.1039/D3BM01039B

23- Figueiredo-Godoi, L. M. A., Garcia, M. T., Pinto, J. G., Ferreira-Strixino, J., Faustino, E. G., Pedroso, L. L. C., & Junqueira, J. C. Antimicrobial Photodynamic Therapy Mediated by Fotenticine and Methylene Blue on Planktonic Growth, Biofilms, and Burn Infections of Acinetobacter baumannii. Antibiotics (Basel, Switzerland).2022; 11(5), 619. https://doi.org/10.3390/antibiotics11050619.

24- Wink, D. A., Hines, H. B., Cheng, R. Y., Switzer, C. H., Flores-Santana, W., Vitek, M. P., Ridnour, L. A., & Colton, C. A. Nitric oxide and redox mechanisms in the immune response. Journal of leukocyte biology.2011; 89(6), 873–891. https://doi.org/10.1189/jlb.1010550

25- Qiu, X., Wu, Y., Zhang, D., Zhang, H., Yu, A., & Li, Z. Roles of oxidative stress and raftlin in wound healing under negative-pressure wound therapy. Clinical, Cosmetic and Investigational Dermatology2021; 1745-1753. http://dx.doi.org/10.2147/CCID.S334248

26- Salih Ağırtaş, M., Karataş, C., & Özdemir, S. Synthesis of some metallophthalocyanines with dimethyl 5-(phenoxy)-isophthalate substituents and evaluation of their antioxidant-antibacterial activities. Spectrochimica acta. Part A, Molecular and biomolecular spectroscopy.2015; 135, 20–24. https://doi.org/10.1016/j.saa.2014.06.139

27- Kalay, Z., & Cevher, S. C. Oxidant and antioxidant events during epidermal growth factor therapy to cutaneous wound healing in rats. International wound journal.2012; 9(4), 362–371. https://doi.org/10.1111/j.1742-481X.2011.00895.x

28- Alemdaroğlu, C., Değim, Z., Celebi, N., Zor, F., Oztürk, S., & Erdoğan, D. An investigation on burn wound healing in rats with chitosan gel formulation containing epidermal growth factor. Burns : journal of the International Society for Burn Injuries.2006; 32(3), 319–327. https://doi.org/10.1016/j.burns.2005.10.015.

29- Güleç Peker, E. G., Coşkun, Ş., Ebegil, M., & Acartürk, F.Effect of exogenous epidermal growth factor (EGF) on nonenzymatic antioxidant capacities and MPO activity of wound tissue. Medicinal Chemistry Research.2010; 19, 533-540. http://dx.doi.org/10.1007/s00044-009-9210-z.

30- Shanmugapriya K, Kim H, Kang HW. EGFR-conjugated hydrogel accelerates wound healing on ulcer-induced burn wounds by targeting collagen and inflammatory cells using photoimmunomodulatory inhibition. Materials Science and Engineering: C. 2021 Jan 1;118:111541

31- Y. Mao, J. Ma, Y. Xia, X. Xie, The Overexpression of Epidermal Growth Factor (EGF) in HaCaT Cells Promotes the Proliferation, Migration, Invasion and Transdifferentiation to Epidermal Stem Cell Immunophenotyping of Adipose-Derived Stem Cells (ADSCs), Int. J. Stem Cells. 13(1) (2020) 93, doi: 10.15283/ijsc18146.